

# Synthesis of Hollow Nanoparticles $\gamma$ -Al<sub>2</sub>O<sub>3</sub>

Dmitry V. Smovzh, Nikolay A. Kalyuzhnyi, Alexey V. Zaikovsky, Sergey A. Novopashin\*

Kutateladze Institute of Thermophysics of Siberian Branch of Russian Academy of Sciences, Novosibirsk, Russia

Email: \*sanov@itp.nsc.ru

Received March 4, 2013; revised April 5, 2013; accepted April 12, 2013

Copyright © 2013 Dmitry V. Smovzh *et al.* This is an open access article distributed under the Creative Commons Attribution License, which permits unrestricted use, distribution, and reproduction in any medium, provided the original work is properly cited.

## ABSTRACT

The formation of hollow nanoparticles of alumina was detected when nanostructured carbon–aluminum material, synthesized by composite electrode sputtering in an electric arc, was annealed in oxygen. The synthesized material was characterized by the methods of transmission electron microscopy, thermogravimetry, and roentgen-phase analysis. It is shown that the alumina is the  $\gamma$ -phase; the typical size of particles is 6 - 12 nm and they have a wall thickness of 2 - 3 nm. The mechanism of formation of the hollow nanoparticles of alumina is suggested.

**Keywords:** Hollow Nanoparticles; Alumina; Arc Discharge

## 1. Introduction

Ceramics based on Al<sub>2</sub>O<sub>3</sub> are widely used by modern industry as a construction material with several unique properties such as high mechanical strength and hardness, heat resistance, chemical inertness, and insulation characteristics. Another important application of materials based on Al<sub>2</sub>O<sub>3</sub> is the creation of various catalytically active complexes for the oil industry and cleaning of industrial emissions.

The main physical and chemical methods used for the synthesis of nanocrystalline materials are described in review [1]. The synthesis of fullerenes [2,3], carbon nanotubes [4], and hollow WS<sub>2</sub> structures by annealing of tungsten films in hydrogen sulfide [5] is among the methods of synthesizing hollow nanoparticles. Technologies based on the Kirkendall effect are also among the methods used for the formation of hollow nanoparticles [6]. This method was used for the synthesis of hollow nanoparticles of NiO, CdS, Co<sub>3</sub>S<sub>4</sub>, CoO, CoSe, CoSe<sub>2</sub>, CoTe, Cu<sub>2</sub>O, ZnS, PbS, Fe<sub>x</sub>O<sub>y</sub>, AuPt, Ni<sub>2</sub>P, Co<sub>2</sub>P, AlN, AlN, SiO<sub>2</sub>, Al<sub>2</sub>O<sub>3</sub>, and others [7-12]. Hollow nanoparticles of different compounds on the micron scale are synthesized by aerosol methods [13], including different phases of alumina [14,15]. It is also necessary to mention the technologies and methods based on electrochemical separation [16].

The application of an electric arc for synthesis of nano-

materials relates to the pioneering work [2] on fullerene synthesis. Then, the same technology was used for synthesis of carbon nanotubes [3]. An electric arc in buffer inert gas at decreased pressure was used for the synthesis of metal-carbon nanoparticles [17-20]. In the current study, plasma-arc technology is used for the synthesis of a alumina nanoparticles. The process was performed in two stages: the first stage is synthesis of aluminum-carbon material; the second stage is annealing of the synthesized material in an oxygen-bearing atmosphere. Annealing allows the removal of carbon matrix and synthesis of a alumina nanoparticles.

## 2. Experiment

Experiments were carried out in the DC electric arc under pressure of buffer gas (helium) of 25 torr at an arc current of 100 A. The sputtered electrode (anode) was made of a metal-carbon composite rod 70 cm in length and 7 mm in diameter with a C:Al weight ratio of 15:1. The sprayed material was deposited on a cooled screen. Then, the synthesized composite material was annealed in air at temperatures of 400°C - 950°C. The synthesized material was analyzed by transmission electron microscopy (TEM), thermogravimetry (TGA), and roentgen-phases analysis (XRD) in the angle range of 10° - 75° with a step of  $2\theta = 0.05^\circ$  and storage time of 3 s at every point; monochromatic CuK $\alpha$  radiation was applied ( $\lambda = 1.5418$  Å).

\*Corresponding author.

### 3. Results

The metal-carbon deposit produced is relatively uniform material. The image of this material obtained via TEM is shown in **Figure 1**.

The TEM pictures of synthesized material do not differ qualitatively from the pictures of material obtained by sputtering of the pure graphite electrode without aluminum. In particular, in the pictures it is impossible to distinguish the outline of separate aluminum particles. The element analysis (EDAX) detected aluminum in the synthesized material, and there were no lines of aluminum crystalline structure in the XRD spectra. The XRD spectra of graphite (1), pure carbon material (2), and aluminum-carbon material (3) obtained by sputtering of graphite (2) and aluminum-carbon (3) electrodes are shown in **Figure 2**. The lines of graphite (C), fullerene phases of carbon (F), and aluminum carbide ( $\text{Al}_4\text{C}_3$ ) are indicated in **Figure 2**.

It can be seen in **Figure 2** that the synthesized material includes the graphite lines and lines corresponding to fullerenes. Moreover, the composite material includes aluminum carbide (curve 3). The above results make it possible to conclude that the synthesized material is an amorphous carbon matrix in which the highly dispersed aluminum introduced is partially or totally in a carbide compound. According to TEM analysis of the images, the typical scale of dispersion does not exceed 1 - 2 nm.

The thermogravimetric analysis was carried out in air at a temperature of up to 1200°C with a linear increase during two hours. According to **Figure 3**, the main loss of mass occurs in the temperature range of 400°C - 800°C. This range includes the oxidation temperatures of all forms of carbon as well as the reaction of aluminum carbide with oxygen at 650°C - 700°C:  $\text{Al}_4\text{C}_3 + 6\text{O}_2 = 2\text{Al}_2\text{O}_3 + 3\text{CO}_2$ . The mass of residual material is 10% - 13% of the initial mass and corresponds to the mass share of aluminum in the initial sample, taking into account its oxidation.

The temperature history of the material's morphology was studied during annealing. The material was annealed in air at 400, 550, 700 and 950°C for 1 hour at every temperature. The TEM images are shown in **Figures 4(a)-(d)** for different annealing temperatures.

During annealing, gradual structurization of the material occurs and at 900°C a significant part of the material is represented by hollow shells. According to the image analysis, with a rise in temperature the shape of the structures in the material becomes more spherical and the typical size of observed carbon structures changes from 10 - 30 nm in the initial material to 6 - 14 nm in alumina after annealing at 950°C. The size distribution of particles measured via TEM image processing is shown in **Figure 5** (shell thickness distribution is shown in the inset).

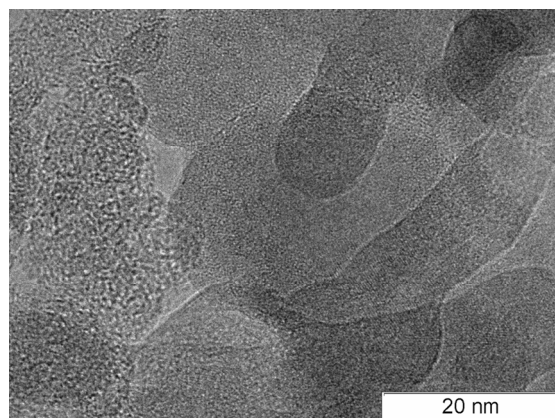


**Figure 1.** TEM of aluminum—carbon composite.

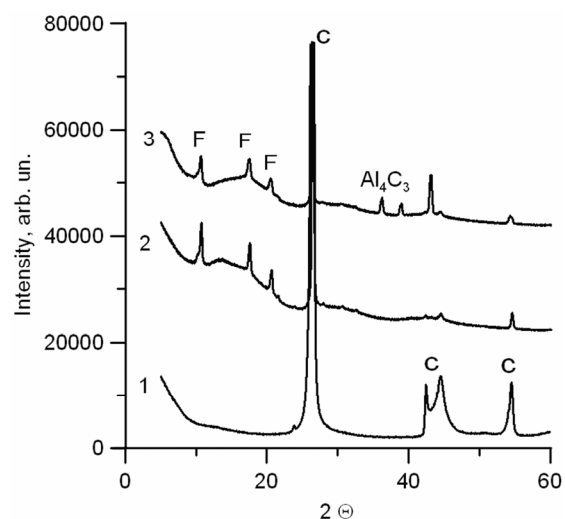


**Figure 2.** XRD spectra. 1-graphite; 2-carbon material, obtained via sputtering of graphite electrode in electric arc; 3-aluminum—carbon material, obtained via spraying of composite electrode in electric arc.

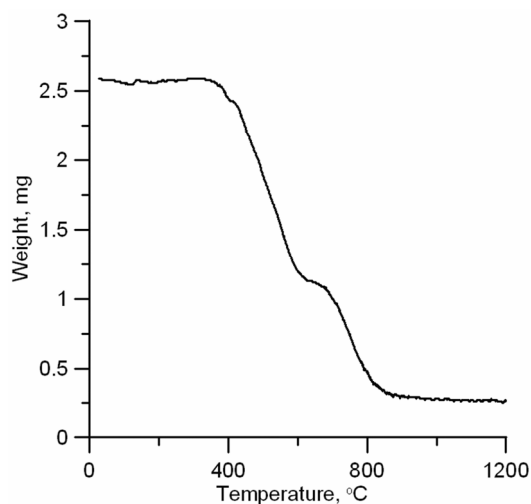


**Figure 3.** TGA analysis of synthesized aluminum carbon sample.

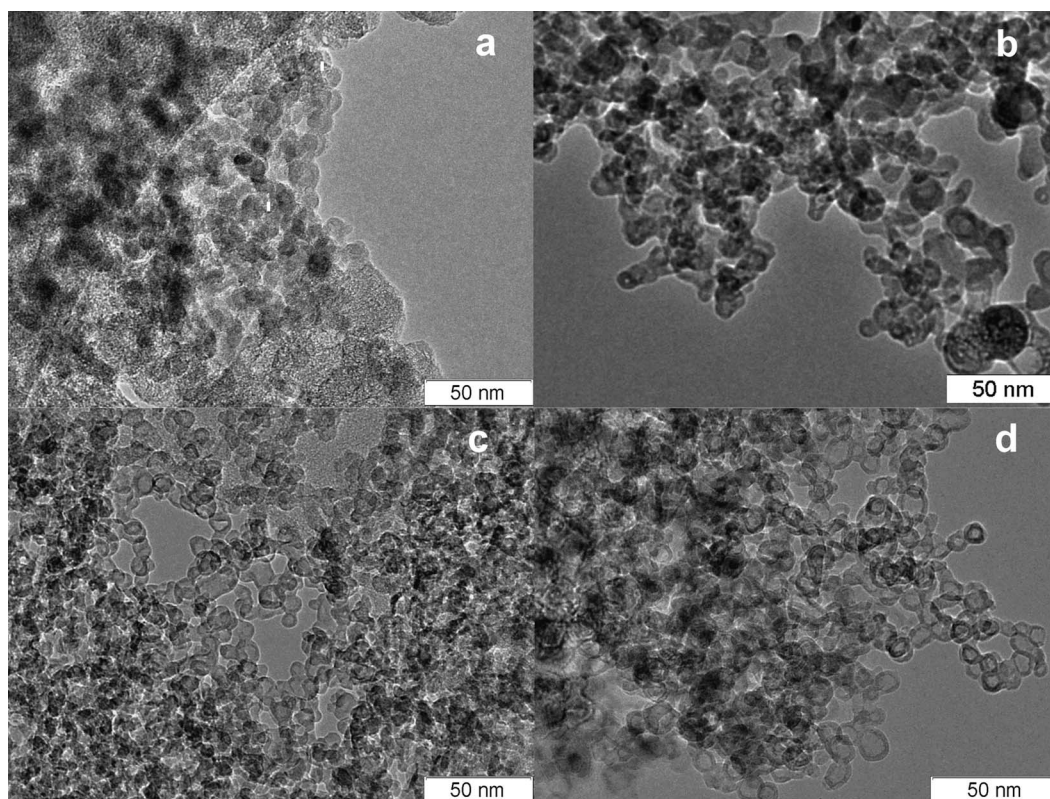


Figure 4. Morphology of material annealed at (a)  $-400^{\circ}\text{C}$ , (b)  $-550^{\circ}\text{C}$ , (c)  $-700^{\circ}\text{C}$ , (d)  $-950^{\circ}\text{C}$ .

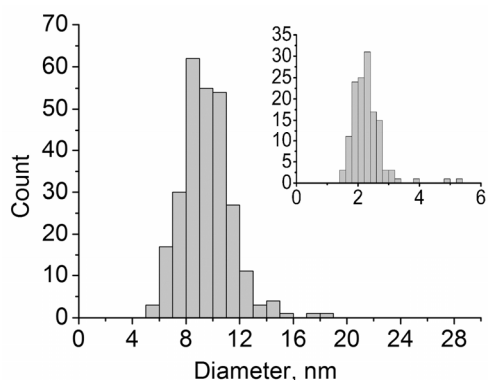


Figure 5. Size distribution of particles. Inset: size distribution of wall thicknesses.

Elemental analysis of the material after annealing shows that there is no carbon in the sample. According to roentgen-phase analysis, the synthesized hollow shells are the  $\gamma$ -phase of alumina. The XRD table data for  $\gamma\text{-Al}_2\text{O}_3$  (curve 1) and synthesized material (curve 2) are compared in **Figure 6**.

The peaks positions of the spectra coincide, that allows concluding that the synthesized material is  $\gamma\text{-Al}_2\text{O}_3$ . The lines spreading in the angle range of  $20 - 50$  result in its overlapping. This phenomenon is obvious due to a small dimension of the coherent region of crystal structure of hollow nanoparticles.

Therefore, plasma-arc synthesis of aluminum—graphite material followed by annealing in an oxygen-bearing atmosphere allowed the synthesis of hollow  $\gamma\text{-Al}_2\text{O}_3$  nanoparticles with a typical size of  $6 - 14$  nm and wall thickness of  $2 - 3$  nm.

One of the most important scientific questions arising from the results of the investigation is the determination of the mechanism of formation of hollow nanoparticles of alumina. According to our studies we suggest the following mechanism. Following the first stage of plasma synthesis by atomic sputtering of aluminum, joint condensation of carbon and aluminum occurs in which aluminum is partially or totally carbided, and the size of crystallites in the synthesized material is no larger than  $2$  nm. The structure of the synthesized material is represented by carbon agglomerates with a typical size of  $15 - 30$  nm (**Figure 1**). On annealing in oxygen, carbon from the agglomerate surface is oxidized, which leads to a decrease in the agglomerates' size and an increase in the aluminum concentration in the surface layers of particles. Simultaneously, aluminum is oxidized, and at temperatures of  $650^{\circ}\text{C} - 700^{\circ}\text{C}$  the reaction of aluminum carbide transformation into oxide occurs. This process takes place until a dense frame of alumina is formed, and then carbon oxidation occurs via oxygen diffusion into the particle and removal of oxidation products (**Figure 7**). According to the estimated elemental composition of the synthesized

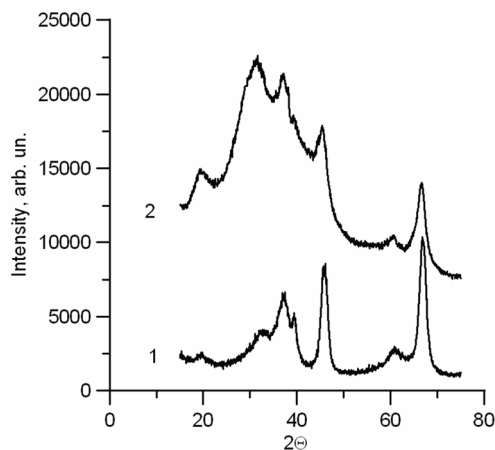


Figure 6. XRD spectra. 1-Table spectrum of  $\gamma$ - $\text{Al}_2\text{O}_3$ ; 2-Synthesized material.

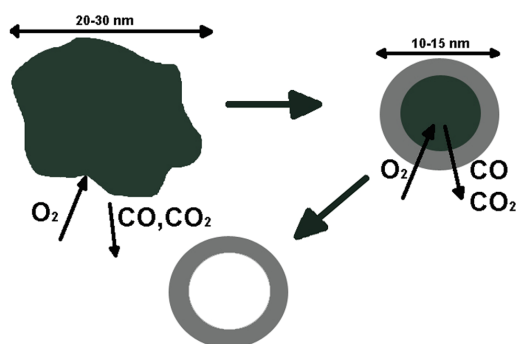


Figure 7. Formation mechanism of hollow nanoparticles of alumina.

material, the initial weight concentration of aluminum of 6.7% in the initial particles of metal-carbon material with a size of 30 nm is equivalent to the amount of aluminum oxide in a spherical hollow particle with a diameter of 10 nm and wall thickness of 2.5 nm; this result agrees with the experimental data.

#### 4. Conclusion

Hollow nanoparticles of  $\gamma$ - $\text{Al}_2\text{O}_3$  were synthesized by the method of electric-arc sputtering of a composite electrode in inert gas followed by oxidation. The effect of the temperature of annealing in an oxygen-bearing atmosphere on the morphology of the synthesized material was analyzed. The mechanism of formation of the hollow nanoparticles was suggested. We can state that this new material is of particular interest for catalytic applications and materials science.

#### 5. Acknowledgements

The work was financially supported by The Ministry of education and science of Russian Federation, State Contract No.11.519.11.5001.

#### REFERENCES

- [1] H. Gleiter, "Nanocrystalline Materials," *Progress in Materials Science*, Vol. 33, No. 4, 1989, pp. 223-315. [doi:10.1016/0079-6425\(89\)90001-7](https://doi.org/10.1016/0079-6425(89)90001-7)
- [2] H. W. Kroto, *et al.*, "C60: Buckminsterfullerene," *Nature*, Vol. 318, No. 14, 1985, pp. 162-163. [doi:10.1038/318162a0](https://doi.org/10.1038/318162a0)
- [3] W. Kratschmer, L. D. Lamb, K. Fostiopoulos and D. R. Hoffman, "Solid C-60-a New Form of Carbon," *Nature*, Vol. 347, No. 27, 1990, pp. 354-358. [doi:10.1038/347354a0](https://doi.org/10.1038/347354a0)
- [4] S. Iijima, "Helical Microtubes of Graphitic Carbon," *Nature*, Vol. 354, No. 6348, 1991, pp. 56-58. [doi:10.1038/354056a0](https://doi.org/10.1038/354056a0)
- [5] R. Tenne, L. Margulis, M. Genut and G. Hodes, "Polyhedral and Cylindrical Structures of Tungsten Disulphide," *Nature*, Vol. 360, No. 6403, 1992, pp. 444-446. [doi:10.1038/360444a0](https://doi.org/10.1038/360444a0)
- [6] H. J. Fan, U. Gesele and M. Zacharias, "Formation of Nanotubes and Hollow Nanoparticles Based on Kirkendall and Diffusion Processes: A Review," *Small*, Vol. 3 No. 10, 2007, pp. 1660-1671. [doi:10.1002/sml.200700382](https://doi.org/10.1002/sml.200700382)
- [7] C. Andreu, K. S. Rachel, Y. Yadong, H. M. Zheng, B. M. Reinhard, H. T. Liu and A. P. Alivisatos, "Sulfidation of Cadmium at the Nanoscale," *ACSNano*, Vol. 2, No. 7, 2008, pp. 1452-1458. [doi:10.1021/nn800270m](https://doi.org/10.1021/nn800270m)
- [8] J. S. Zhou, L. L. Ma, H. H. Song, B. Wu and X. H. Chen, "Durable High-Rate Performance of CuO Hollow Nanoparticles/Graphene-Nanosheet Composite Anode Material for Lithium-Ion Batteries," *Electrochemistry Communications*, Vol. 13, No. 12, 2011, pp. 1357-1360. [doi:10.1016/j.elecom.2011.08.011](https://doi.org/10.1016/j.elecom.2011.08.011)
- [9] J. G. Railsback, A. C. Johnston-Peck, J. W. Wang and J. B. Tracy, "Size-Dependent Nanoscale Kirkendall Effect During the Oxidation of Nickel Nanoparticles," *ACSNano*, Vol. 4, No. 4, 2010, pp. 1913-1920. [doi:10.1021/nn901736v](https://doi.org/10.1021/nn901736v)
- [10] J. X. Wang, C. Ma, Y. M. Choi, D. Su, Y. M. Zhu, P. Liu, R. Si, M. B. Vukmirovic, Y. Zhang and R. R. Adzic, "Kirkendall Effect and Lattice Contraction in Nanocatalysts: A New Strategy to Enhance Sustainable Activity," *Journal of the American Chemical Society*, Vol. 133, No. 34, 2011, pp. 13551-13557. [doi:10.1021/ja204518x](https://doi.org/10.1021/ja204518x)
- [11] R. Nakamura, D. Tokozakura, H. Nakajima, J.-G. Lee and H. Mori, "Hollow Oxide Formation by Oxidation of Al and Cu Nanoparticles," *Journal of Applied Physics*, Vol. 101, 2007, Article ID: 074303.
- [12] B. Koo, H. Xiong, M. D. Slater, V. B. Prakapenka, M. Balasubramanian, P. Podsiadlo, C. S. Johnson, T. Rajh and E. V. Shevchenko, "Hollow Iron Oxide Nanoparticles for Application in Lithium Ion Batteries," *Nano Letters*, Vol. 12, No. 5, 2012, pp. 2429-2435. [doi:10.1021/nl3004286](https://doi.org/10.1021/nl3004286)
- [13] C. Roth and R. Koebrich, "Production of Hollow Spheres," *Journal of Aerosol Science*, Vol. 19, No. 7, 1988, p. 939.
- [14] J. H. Nadler, T. H. Sanders and J. K. Cochran, "Aluminum Hollow Sphere Processing Materials," *Science Forum-Trans Tech Publications (Switzerland)*, Vol. 331, No. 1, 2000, pp. 495-500.

- [15] A. Kato and Y. Hirata, "Sintering Behaviour of Beta-Type Alumina Powders Prepared by Spray-Pyrolysis Technique and Electrical Conductivity of Sintered Body," *Kyushu University*, Vol. 45, No. 4, 1985, p. 251.
- [16] S. J. Bae, J. S. Yoo, Y. Lim, S. Kim, Y. C. Lim, K. S. Nahm, S. J. Hwang, T.-H. Lim, S.-K. Kim and P. Kim, "Facile Preparation of Carbon-Supported PtNi Hollow Nanoparticles with High Electrochemical Performance," *Journal of Materials Chemistry*, Vol. 22, No. 18, 2012, pp. 8820-8825. [doi:10.1039/c2jm16827h](https://doi.org/10.1039/c2jm16827h)
- [17] J. H. J. Scott and S. A. Majetich, "Morphology, Structure, and Growth of Nanoparticles Produced in a Carbon Arc," *Physical Review B*, Vol. 52, No. 17, 1995, pp. 12564-12571. [doi:10.1103/PhysRevB.52.12564](https://doi.org/10.1103/PhysRevB.52.12564)
- [18] V. A. Maltsev, S. A. Novopashin, O. A. Nerushev, S. Z. Sakhapov and D. V. Smovzh, "Synthesis of Metal Nanoparticles on the Carbon Substrate," *Nanotechnologies in Russian*, Vol. 2, No. 5-6, 2007, pp. 85-89.
- [19] J. Borysiuka, A. Grabiasa, J. Szczytkob, M. Bystrzejewskic, A. Twardowskib and H. Lange, "Structure and Magnetic Properties of Carbon Encapsulated Fe Nanoparticles Obtained by Arc Plasma and Combustion Synthesis," *Carbon*, Vol. 46, No. 13, 2008, pp. 1693-1701. [doi:10.1016/j.carbon.2008.07.011](https://doi.org/10.1016/j.carbon.2008.07.011)
- [20] J.-C. Lo, J.-C. Lu and M.-H. Teng, "A New Crucible Design of the Arc-Discharge Method for the Synthesis of Graphite Encapsulated Metal (GEM) Nanoparticles," *Diamond & Related Materials*, Vol. 20, No. 3, 2008, pp. 330-333. [doi:10.1016/j.diamond.2011.01.029](https://doi.org/10.1016/j.diamond.2011.01.029)